High-resolution multidimensional displacement monitoring system

Neville K. S. Lee
Yimin Cai
Ajay Joneja
Hong Kong University of Science and Technology
Department of Industrial Engineering & Engineering Management
Clear Water Bay
Kowloon, Hong Kong
E-mail: nlee@usthk.ust.hk

Abstract. The possibility of using quadrant detectors to develop a new optical system that can monitor all six degrees of freedom of mechanical workpieces with very high resolution is investigated. A prototype system based on this approach has been designed and built. Although the system is not fully optimized, our proposed system has already demonstrated some promising results. Using a thermally compensated laser source together with a pinhole spatial filtering system, we have demonstrated that lateral resolution better than 50 nm and angular displacement resolution better than 0.25 μrad is achievable with this system.
 [S0091-3286(97)04008-7]

Subject terms: precision setups; displacement monitors; quadrant detectors.

Paper 05126 received Dec. 2, 1996; revised manuscript received March 19, 1997; accepted for publication April 7, 1997.

1 Introduction

There are many applications in which very precise noncontact displacement measurements are needed. Some of the noncontact methods include interferometers,[1,2] optical probes,[3,4] and triangulation.[5] One common feature of these techniques is that they measure displacement in the direction of the optical axis of the system. Recently, an interesting high-resolution lateral displacement sensing method was proposed by Makynen et al.[6] In their approach, a cooperative illuminated target such as a rectangular reflector is reimaged onto a quad detector. The quad detector, which acts as a two-dimensional position detector, can then track the two lateral displacements of the target perpendicular to the optical axis.

While Makynen's approach can monitor lateral displacement of an object perpendicular to the optical axis, there are some applications that may require monitoring displacement of an object along all three orthogonal axes (that is, perpendicular to and along the optical axis). In addition to the lateral displacement, these applications may also require monitoring the rotational displacement. We have recently performed some experiments to investigate manufacturing processes using a mechanical alignment method[7,8] that is widely used in industry. Position repeatability experiments on locating a workpiece with respect to a set of datum surfaces were carried out to determine the level of manufacturing precision that can be supported by this method. The factors that can affect the manufacturing precision of such a process were also studied, leading to the development of methods to suppress the effect of these factors. In order to monitor the positioning repeatability of the workpiece, we have to monitor both the lateral displacement and the rotational displacement. A new high-resolution system that can measure multidimensional rotational and lateral displacements has been developed for this purpose.

We took a somewhat different approach than the Makynen et al. Instead of an illuminated target, we use a laser beam, multiple prisms, and multiple quad detectors. Our approach allows us to simultaneously monitor multidimensional rotational and lateral displacements. As discussed later in this paper, the spot size on the quad detector is one important factor determining the resolution of the system. In comparison with reimaging an illuminated target, a focused laser beam can provide a much smaller spot size with much higher light intensity. Therefore, potentially, much higher displacement resolution can be achieved with our approach.

In this paper, we will first describe the design of our multidimensional displacement monitoring system. Then we will discuss the performance characteristics of our detection system at each quad detector. Lateral displacement sensitivity on the order of 100 nm and rotational displacement sensitivity of 0.05 arcsec (0.2 μrad) have been achieved. An analysis of the system's performance was performed, based on the single-quad-detector performance.

While the implementation of our approach may appear to be quite straightforward, a few subtle design considerations are required to achieve optimality. As shown in the appendix, another, similar design yields a two-order-of-magnitude poorer resolution than our current design.

2 Design of the Multidimensional Monitoring System

A schematic of the multidimensional monitoring system that we propose is shown in Fig. 1. The figure shows a rectangular workpiece located via a 3-2-1 scheme (only the two pins of the secondary datum and the one pin of the tertiary datum are shown). Two split prisms, P_2 and P_3, are attached to the workpiece. A collimated laser beam is split via the fixed prism P_1 into two beams. The first beam is directed, via mirrors M_2 and M_3, to the reflection prism P_3 mounted on the workpiece. The reflected beam goes through a lens L_2, which focuses the laser beam onto quad detector D_3. The second laser beam will first go through a lens L_1 before being split two ways via prism P_2 on the

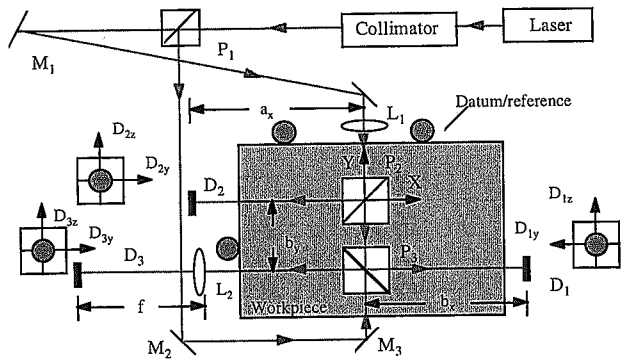

Fig. 1 The 5-D monitoring system.

workpiece. The reflected beam is directed to quad detector D_2. The transmitted beam hits the reflection prism P_3 and is directed to quad detector D_1. Both quad detectors D_1 and D_2 are located at the focal point of lens L_1.

Any displacement of the workpiece will change the orientation and/or the lateral position of the prism that reflected the laser beam. This will cause the laser beam to move across the quad detectors. The principle of position detection of laser-beam movements by the quad detector is well known.[9,10] The photosensitive sensor area is divided into four quadrants, each of which generates a voltage output depending on the intensity of illumination incident upon it. If the laser spot moves from the left side to the right side of the quad detectors, the output from the left-side detectors decreases while the output from the right-side detectors increases. The differential output (left-side detector minus right-side detector) accordingly changes.

Figure 1 shows a schematic arrangement of our multidimensional detection system. We would like to highlight an important feature of this arrangement: since D_3 is at the focal point of lens L_2, the position of the focus spot of the laser beam on D_3 is not sensitive to the lateral displacement of the laser beam due to the lateral displacements (that is, the X, Y, or Z translations) of the reflecting prism P_3. Therefore, any deflection of the laser beam at D_3 is purely due to rotational component of the workpiece displacement. This isolated measurement of the rotations of the workpiece can then be used to calculate accurately the translations of the workpiece based on the readings of detectors D_1 and D_2.

In principle, a simpler arrangement is sufficient to detect multidimensional lateral and rotational displacement, as shown in the appendix. In that arrangement, there is no special feature to decouple the measurement of rotational displacements from the lateral displacements. Thus (refer to appendix) all the deflections measured at the detectors are due to the combined effects of rotation and translation of the workpiece. But, as shown by the calculations, the performance of that arrangement is significantly worse than that of the arrangement shown above. Our empirical data show that the latter system's performance is approximately two orders of magnitude worse.

The general expression of the relationship between the displacement of the workpiece and the movement of the laser beams on the three quad detectors can be quite complicated. But since we are more interested in high resolution of small displacements, we can use small-angle approximations, which lead to greatly simplified expressions, especially with all the normal incidences and reflected laser beams from prism P_2 and P_3 propagating along the x and y axes. In the approximation of small angular and lateral displacements, the relationship between the displacement of the workpiece and the movement of the laser beams on the three quad detectors can be expressed as follows:

$$D_{1y}=(b_y+2b_x)\theta_z+\Delta x+\Delta y, \tag{1}$$

$$D_{1z}=(b_x+b_y)\theta_x-b_x\theta_y, \tag{2}$$

$$D_{2y}=-2a_x\theta_z-\Delta x+\Delta y, \tag{3}$$

$$D_{2z}=a_x\theta_x+a_x\theta_y, \tag{4}$$

$$D_{3y}=-f\times 2\theta_z, \tag{5}$$

$$D_{3z}=-f\theta_x+f\theta_y, \tag{6}$$

$$a_x=b_x+b_y. \tag{7}$$

Here D_{1y}, D_{2y}, and D_{3y} are the horizontal displacements of the focused laser beam on quad detectors D_1, D_2, and D_3, respectively; D_{1z}, D_{2z}, and D_{3z} are the vertical displacements of the focused laser beam on the same quad detectors; and θ_x, θ_y, and θ_z are the rotations of the workpiece about the x, y, and z axes, respectively. The origin of the coordinates has been chosen as the center of prism P_2 as shown in Fig. 1, and Δx, Δy, and Δz are the lateral displacements of the workpiece along the x, y, and z axes. The standard right-handed coordinate system is assumed. The linear distances a_x, b_x, and b_y between components are as shown in Fig. 1; f is the focal length of lens L_2. From the above expressions, we can easily derive the following displacement components of the workpiece:

$$\Delta x=0.5\left[D_{1y}-D_{2y}+\frac{(b_x+3a_x)D_{3y}}{2f}\right], \tag{8}$$

$$\Delta y=0.5\left[D_{1y}+D_{2y}-\frac{b_yD_{3y}}{2f}\right], \tag{9}$$

$$\theta_x=0.5\left(\frac{D_{2z}}{a_x}-\frac{D_{3z}}{f}\right), \tag{10}$$

$$\theta_y=0.5\left(\frac{D_{2z}}{a_x}+\frac{D_{3z}}{f}\right), \tag{11}$$

$$\theta_z=-\frac{D_{3y}}{2f}. \tag{12}$$

The system as shown in Fig. 1 can detect five degrees of freedom of the workpiece. Because of the orientation of prisms P_2 and P_3, lateral displacement in the z direction of the workpiece would not result in movement of the reflected laser beam. In other words, our system as shown in

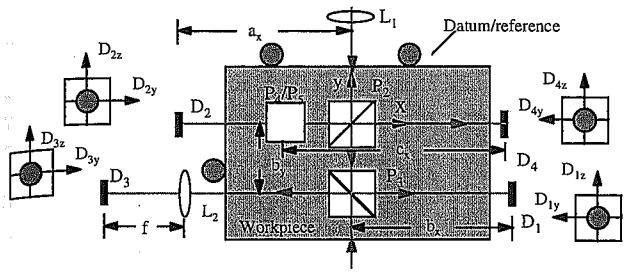

Fig. 2 A 6-D monitoring system.

Fig. 1 is not sensitive to the z-direction lateral displacement. To sense the z-direction lateral displacement, one approach is to change the orientation of the reflected prism P_2 so that the normal axis of the reflecting surface has a z component also. Then lateral displacement of the workpiece would also be translated into lateral displacement in the z direction of the laser spot on D_1 and D_2. However, now the reflected laser beam will not be in the XY plane any more. This makes the system more cumbersome to build and to align, and also would make relationship between D_{1y}, D_{1z}, D_{2y}, D_{2z}, D_{3y}, D_{3z} and Δx, Δy, Δz, θ_x, θ_y, θ_z much more complicated. Since prisms and quad detectors are cheap, we prefer another approach, using additional prisms and detectors, for the 6-D monitoring system. In this approach, as shown in Figs. 2 and 3, two additional prisms P_4 and P_5 and one additional detector D_4 are put on the original 5-D system. Since we have not changed other parts of the optical system, the relations described by Eqs. (1) through (12) still hold. The additional relationship between displacement of the beams on the detector and the lateral displacement Δz is the following:

$$D_{4z}=2\,\Delta z-c_x\theta_y\,. \tag{13}$$

Using Eq. (11), Eq. (13) can be changed into

$$D_{4z}=2\,\Delta z-0.5c_x\left(\frac{D_{2z}}{a_x}+\frac{D_{3z}}{f}\right), \tag{14}$$

where c_x is distance between the prism P_5 and detector D_4, and D_{4z} is the vertical displacement of the focused laser beam on D_4.

3 Performance Characteristics of the Optical System at a Single-Quad-Detector Level

As discussed above, our multidimensional detection system offers a choice of two types of optical arrangements. Both type of arrangements involve a lens focusing a collimated laser beam onto a position-sensitive quad detector. Therefore, as we will discuss in the next section, the system performance can be deduced from the performance characteristics at a single-quad-detector level.

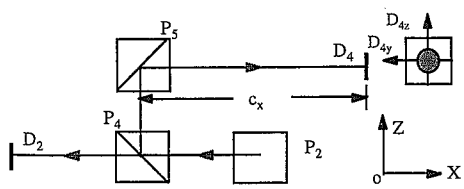

Fig. 3 Cross-section view of the 6-D monitoring system of Fig. 2.

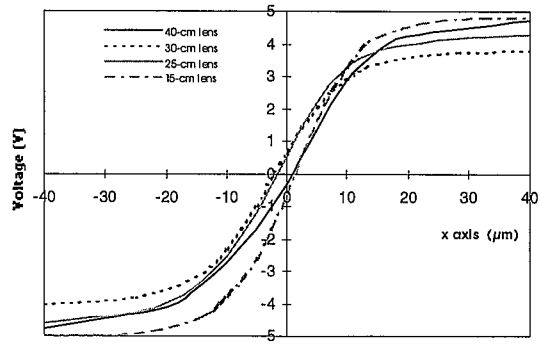

Fig. 4 Calibration curves of quad detector with different lenses.

The position response of the quad detector as a function of focal length of the lens is shown in Fig. 4 and Table 1. As seen in Fig. 4, the most sensitive part of the curve (the steepest part, with the biggest change of signal per unit displacement) is at the zero crossing, where the beam is equally distributed on both side of the detector as shown in Fig. 5. This is because the intensity of the laser spot on the detector has a Gaussian distribution, and the intensity of the center portion of the beam is higher than at the periphery. The shifting of the central portion of the beam causes bigger changes in the power reading of the two halves of the detectors. Therefore we should operate close to the zero crossing to get the maximum sensitivity.

Based on the data shown in Fig. 4 and Table 1, we can plot the sensitivity of the optical system as a function of the focal length as shown in Fig. 6. An optical system with the shorter-focal-length lens has, in general, better sensitivity than an optical system with the longer-focal-length lens. This is because for a given diameter of the collimated beam, the shorter focal length will result in a smaller spot size. The dotted line in Fig. 6 shows that the diameter of the beam calculated from the data in Table 1 indeed increases

Table 1 Data on the curves in Fig. 4.

	Voltage (V)			
x (μm)	40-cm lens	30-cm lens	25-cm lens	15-cm lens
−40	−4.782	−4.040	−4.600	−4.950
−25	4.286	−3.797	−4.309	−4.900
−15	−3.544	−3.185	−3.424	−4.460
−10	−2.740	−2.322	−2.572	−3.786
−5	−1.720	−0.988	−1.227	−2.629
0	−0.327	0.709	0.504	−0.662
5	1.347	2.039	2.209	1.656
10	2.855	2.897	3.261	3.281
15	3.765	3.401	3.762	4.184
25	4.365	3.729	4.095	4.737
40	4.718	3.780	4.300	4.820

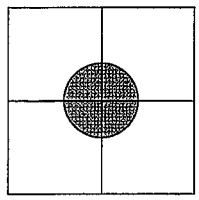

Fig. 5 Central incidence of laser beam on the quad detector.

linearly with the focal length of the lens (correction factors due to the geometry of the quad detector have not been included). Intuitively, a smaller spot size would yield higher sensitivity than a large one because any incremental displacement would mean that a bigger portion of the beam of would be shifted from one half of the quad detector to the other half. This in turn manifests itself in a bigger change in the differential output of the signal. Therefore one should select the shortest-focal-length lens and largest collimated beam consistent with the constraints, such as the sample size to be monitored.

In Table 2 and Fig. 7, we show the response of the optical system with a 25-cm-focal-length lens as a function of laser beam power. It is interesting to note that the amplitude of the response increases initially as the power increases. However, as the power level goes beyond 30 μW under the tight focusing conditions, the response of the detector become nonlinear. As one increases the laser power further, the signal level of the detector decreases and exhibits some oscillation. In Fig. 8, we deduce the sensitivity of the optical system with a 25-cm-focal-length lens as a function of power, based on response data shown in Fig. 7 and Table 2. It was found that this nonlinear effect depends on the intensity of the beam and not the total power of the beam. Therefore, the optimum value for the input laser depends on the spot size on the detector. As discussed later, the noise level also depends on the laser power. Since our ultimate goal is high resolution, the selection of the optimum power of the laser should be based on the resolution, which requires us to take the nonlinear response to the noise into account.

As the resolution depends not only on the sensitivity but also the noise level of the system, considerable effort was put into controlling the noise. To minimize the noise, our experiment was set up in a controlled environment. The monitoring system was set on a vibration-controlled optical table (Newport model RS2000™) inside

Table 2 Data on the curves in Fig. 7.

	Voltage (V)				
x (μm)	56 μW	45.2 μW	31.5 μW	24.2 μW	17.1 μW
−40	−1.490	−4.212	−5.000	−4.150	−3.640
−30	−1.362	−3.927	−4.862	−4.204	−3.458
−20	−1.100	−3.507	−4.489	−4.085	−3.122
−10	−0.335	−2.109	−2.773	−3.674	−2.246
0	−0.003	0.467	1.284	−0.729	0.768
10	0.351	2.431	4.077	3.012	2.726
20	0.766	3.368	4.633	4.022	3.028
30	0.828	3.785	4.817	4.159	3.228
40	0.964	3.863	4.888	4.182	3.325

a temperature-controlled room. The temperature was kept constant within 1°.

There are many potential sources of noise in our monitoring system. First we characterized background electrical noise, which was found to be less than 0.0005 V. Based on the sensitivity of 0.2 to 0.4 V/μm for our system (using 15- to 25-cm-focal-length lenses), this electric noise contributes the equivalent of about 2 to 3 nm in uncertainty of measurement. Another potential source of noise was the ambient lighting, which may fluctuate an induce some noise via the quad detectors. However, since the ambient light fluctuation most likely affects all four quadrants of the quad detector equally, this noise should cancel out in the differential output of the quad detectors. Indeed, we found that this kind of noise contributes less than 1 nm of uncertainty in our system.

Perhaps the major source of noise for our system came from the shifting of direction of laser beam, which causes fluctuations in the differential output signal of the quad detector. Originally, a Newport model U1335 He-Ne laser was used. The resolution achievable by our monitoring system using this laser source ranged from 2 to 4 μm. To reduce the laser noise problem, we first replaced the Newport laser with a thermally compensated Spectral Physics model 117 He-Ne laser. In the intensity-stabilized mode, its intensity stability over an hour is less than ± 0.1%. In addition, we have implemented a pinhole filter system to suppress some of the parasitic higher-order modes.[11] The prob-

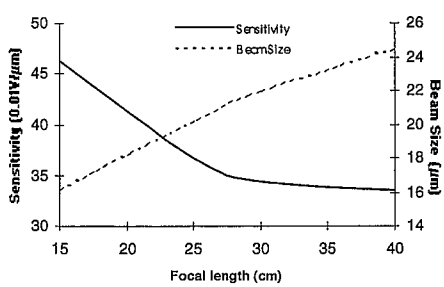

Fig. 6 Sensitivities and beam sizes under different lenses.

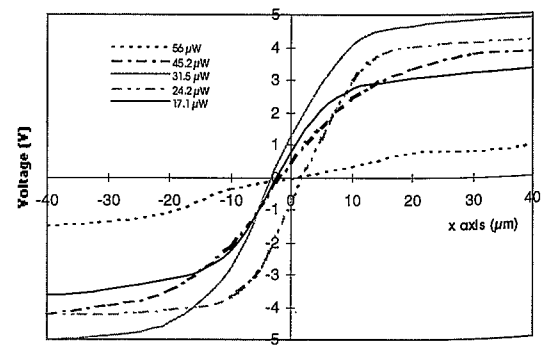

Fig. 7 Calibration curves of quad detector at different laser powers.

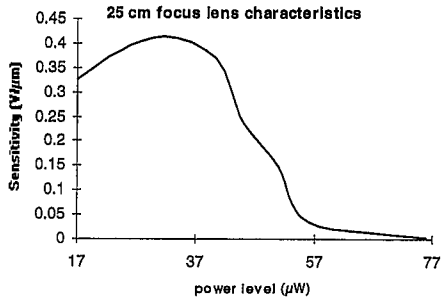

Fig. 8 Relationship between sensitivity and laser power level.

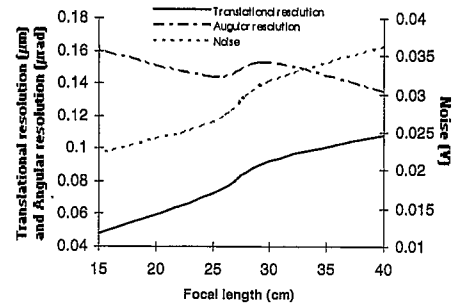

Fig. 9 Resolution and noise levels with different lenses.

lem with the higher-order modes is that they compete with each other and the laser map hop between them, which results in shifting of the laser propagation direction. Shifting of the laser beam would result in undesirable laser displacement across the detectors.

With the new laser system, the noise level of our system is substantially reduced. The noise and the resolution using the new laser system are summarized in Table 3 and Figs. 9 and 10. Here the resolution is defined as the uncertainty of displacement measurement at 1σ (one standard deviation) of noise. As shown in Table 3, the resolution for lateral displacement improves as the focal length decreases, and the best lateral resolution is about 50 nm using a 15-cm-focal-length lens. But for angular displacement, the resolution is nearly constant, with a slight improvement using the longer-focal-length lens system. This is because for a given angular displacement, the lateral displacement of the laser spot across the detector is proportional to the focal length of the detector. The best angular resolution is about 0.14 μrad using a 40-cm lens.

4 Performance of the Multidimensional System

Based on the performance data on the optical system at a single-quad-detector level, we can estimate the performance characteristics of the multidimensional monitoring system according to Eqs. (8) to (13). Since we have common laser noise sources, strictly speaking the noise sources for D_{1y}, D_{1z}, D_{2y}, D_{2z}, D_{3y}, D_{3z} are related to each other. Unfortunately, our electronics do not allow us to take data simultaneously (which would allow us to cancel out some of the noise factors). As we do not take the data on each variable at exactly the same time, we treat D_{1y}, D_{1z}, D_{2y}, D_{2z}, D_{3y}, D_{3z} as independent variables. Since Eqs. (8) to (12) and (14) are linear equations, the resolution of the system becomes

$$R_{\Delta x}=\left[(0.5\sigma_{1y})^2+(0.5\sigma_{2y})^2+0.5^2\left(\frac{b_x+3a_x}{2f}\right)^2\sigma_{3y}^2\right]^{1/2}, \tag{15}$$

$$R_{\Delta y}=\left[(0.5\sigma_{1y})^2+(0.5\sigma_{2y})^2+0.5^2\left(\frac{b_y}{2f}\right)^2\sigma_{3y}^2\right]^{1/2}, \tag{16}$$

$$R_{\Delta z}=\left[\left(\frac{\sigma_{4z}}{2}\right)^2+\left(\frac{c_x\times R_{\theta y}}{2}\right)^2\right]^{1/2}$$

$$=\left[\left(\frac{\sigma_{4z}}{2}\right)^2+\left(\frac{c_x\times\sigma_{2z}}{4a_x}\right)^2+\left(\frac{c_x\times\sigma_{3z}}{4f}\right)^2\right]^{1/2}, \tag{17}$$

$$R_{\theta x}=\left[\left(0.5\,\frac{\sigma_{2z}}{a_x}\right)^2+\left(0.5\,\frac{\sigma_{3z}}{f}\right)^2\right]^{1/2}, \tag{18}$$

$$R_{\theta y}=\left[\left(0.5\,\frac{\sigma_{2z}}{a_x}\right)^2+\left(0.5\,\frac{\sigma_{3z}}{f}\right)^2\right]^{1/2}, \tag{19}$$

$$R_{\theta z}=\left[\left(\frac{\sigma_{3y}}{2f}\right)^2\right]^{1/2}=\frac{\sigma_{3y}}{2f}. \tag{20}$$

For example, our present system has 15 cm as the focal length for L_1 and 40 cm for L_2, $b_y=25$ mm, $b_x = 100$ mm, $a_x = 125$ mm, $c_x = 100$ mm, so, according to Eqs. (8) to (13), the resolution of Δx, Δy, Δz, $\theta_x, \theta_y, \theta_z$ are as follows:

$$R_{\Delta x}=0.047\ \mu\text{m}, \quad R_{\Delta y}=0.034\ \mu\text{m},$$

Table 3 System performance with lenses of various focal lengths.

Focal length (cm)	Sensitivity (V/μm)	Noise (V)	Lateral resolution (μm)	Angular resolution (μrad)
40	0.335	0.036	0.108	0.136
30	0.344	0.032	0.092	0.154
25	0.366	0.027	0.072	0.145
15	0.464	0.022	0.048	0.160

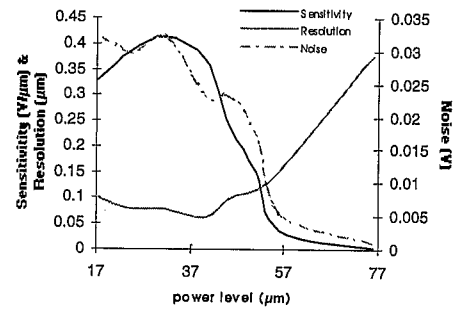

Fig. 10 Sensitivity, resolution, and noise levels at different laser powers.

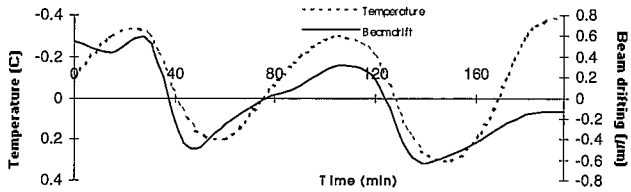

Fig. 11 Thermal-drifting results.

$R_{\Delta z}=0.029\ \mu\text{m}, \quad R_{\theta x}=0.235\ \mu\text{rad},$

$R_{\theta y}=0.235\ \mu\text{rad}, \quad R_{\theta z}=0.135\ \mu\text{rad}.$

5 Thermal Drifting

At such a high resolution in the submicron range, thermal drifting of the system becomes important. The drifting of the laser beam with the 25-cm focal length is shown in Fig. 11. The maximum drifting is about $\pm$ 0.6 μm. The drift figures match well with the fluctuations in temperature of the room, which is periodic.

Since the thermal drifting can be extrapolated, for our own application we took thermal-drifting data in between each displacement measurement. This way we substantially reduced the effect due to thermal drifting.

6 Conclusion

A new optical monitoring system using quad detectors has been developed. The methodology is capable of monitoring all six degrees of freedom of a workpiece. We also present a configuration for monitoring five degrees of freedom (three translation and two rotation) of a workpiece. Based on performance data for a single quad detector, the system is estimated to have lateral resolution in the order of 50 nm and a rotational resolution of 0.25 μrad.

The system is simple to set up, and will be useful for applications requiring alignment and positioning for precision manufacturing. Several issues related to the operation of the device have been studied and discussed, including various sources of noise and methods for noise reduction, thermal effects, etc. We are in the process of investigating how we can further improve the resolution of our system, and to reduce the thermal drifting problem. In addition, we are investigating the behavior of the system for different applications, including studies on accuracy and repeatability of location using mechanical datums, effects of operating environments (such as dust particles), etc.

7 Appendix: Performance Characteristics of a Multidimensional Monitoring System with Coupled Rotation and Translation Effects

As described in Sec. 2 there are different ways to implement a multidimensional monitoring system. An alternative arrangement is shown in Fig. 12. This system is a little bit simpler and easier to implement than the system we propose in Fig. 1.

It is interesting to compare the performance of these two systems. For clarity and ease of comparison, we will restrict ourselves to displacements in the XY plane. The relationship between (D_{1y},D_{2x},D_{3y}) and $(\theta_z,\Delta x,\Delta y)$ can be found easily, as shown below:

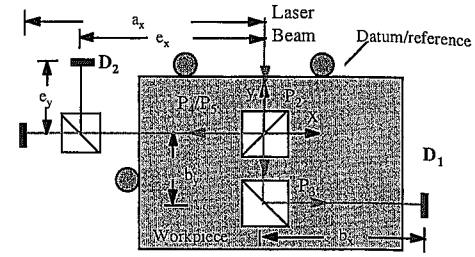

Fig. 12 Monitoring system using the alternative arrangement.

$$D_{1y}=(b_y+2b_x)\theta_z+\Delta x+\Delta y, \tag{21}$$

$$D_{2x}=2(e_x+e_y)\theta_z+\Delta x-\Delta y, \tag{22}$$

$$D_{3y}=-2a_x\theta_z-\Delta x+\Delta y. \tag{23}$$

From the above, simple algebraic manipulation yield the expressions for workpiece displacements at the origin:

$$\Delta x=0.5[D_{1y}-D_{3y}-\theta_z(2a_x+b_y+2b_x)], \tag{24}$$

$$\Delta y=0.5[D_{1y}+D_{3y}-\theta_z(2b_x+b_y-2a_x)], \tag{25}$$

$$\theta_z=0.5\times\frac{D_{2x}+D_{3y}}{e_x+e_y-a_x}. \tag{26}$$

We can estimate the performance characteristics of this monitoring system. For example, our present system has 15-cm focal length, b_y = 25 mm, b_x = 100 mm; according to Eqs. (15) to (20) with the single-detector resolution values we obtained in experiment, the resolutions of $\Delta x,\Delta y,\theta_z$ of this system when the separation between D_2 and D_3 is 2, 4, and 8 mm are as shown in Table 4. The best resolution is around 4-mm separation. When the separation increases further, the resolution of the system becomes worse due to the increasing size of the laser beam.

The problem with this configuration is that the rotational measurement θ_z depends on the separation of quad detectors D_1 and D_2. If the separation of the detectors is small, the sensitivity of the angular displacement is small. But on the other hand, if the separation is large, then one or both of the detectors will be far away from the focal point of the focusing objective lens in this agreement. Thus the spot size on the detector will be large, and the detector is not sensitive to the displacement of the beam. Even with reasonable optimization of the separation of the detectors (for

Table 4 System resolution with various separations between D_2 and D_3.

Separation of D_2 and D_3 (mm)	R_{D1y} (μm)	R_{D2x} (μm)	R_{D3y} (μm)	$R_{\Delta x}$ (μm)	$R_{\Delta y}$ (μm)	$R_{\theta z}$ (μrad)
2	0.048	>0.048	>0.048	>5.7	>0.30	>24
4	0.048	0.08	0.08	4.93	0.26	20.75
8	0.048	0.20	0.20	5.94	0.32	25

example, a system with 15-cm lens focal length and 4-mm separation between D_2 and D_3), the result is about two orders of magnitude worse in angular resolution than for the first arrangement (see Table 4). From Eq. (22), the lateral displacement D_x, which strongly depends on the measured resolution of θ_z, would also have been resolution about two orders of magnitude worse than the performance of the system in Fig. 1. It is therefore clear that the system in Fig. 12 would only be selected if the required resolution was significantly worse than the resolution attainable using the configuration in Fig. 1.

Acknowledgments

We extend our deep appreciation to Mr. Alfred Wong and Mr. K. K. Yung, who spent a lot of time in setting up the equipment and collecting data. We wish to acknowledge the encouragement and support of Professor Mitchell M. Tseng, head of the Department of Industrial Engineering & Engineering Management, Hong Kong University of Science and Technology.

References

1. W. Z. L. Zhuang, J. P. Baird, H. M. Williamson, and R. K. Clark, "Three dimensional displacement measured by a holospeckle interferometer method," *Appl. Opt.* **32**, 4728–4737 (1993).
2. L. M. Smith and C. C. Dobson, "Absolute displacement measurements using modulation of the spectrum of white light in a Michelson interferometer," *Appl. Opt.* **28**, 3339–3342 (1989).
3. W. Wang and I. J. Busch-Vishniac, "The linearity and sensitivity of lateral effect position sensitive devices—an improved geometry," *IEEE Trans. Electron Devices* **36**(11), 2475–2480 (Nov. 1989).
4. Hillmann, "Surface profiles obtained by means of optical methods—are they true representations of the real surface?," *Ann. CIRP*. **39**(1), 581–583 (1990).
5. R. A. Jarvis, "A perspective on range finding techniques for computer vision," *IEEE Trans. Pattern Anal. Machine Intell.* **PAMI-5**, 122–139 (Mar. 1983).
6. A. J. Makynen, J. T. Kostamovaara, and R. A. Myllyla, "A high-resolution lateral displacement sensing method using active illumination of a cooperative target and focused four-quadrant position-sensitive detector," *IEEE Trans. Instrum. Meas.* **44**, 46–52 (1995).
7. N. Lee and A. Joneja, "A methodology to improve manufacturing precision in the presence of workpiece imperfections," *JSME* (Aug. 1997).
8. N. Lee, Y. Cai, and A. Joneja, "Performance of mechanical alignment system in a controlled environment," Private Communication, Hong Kong University of Science and Technology, Dept. of Industrial Engineering and Engineering Management (Dec. 1995).
9. A. J. Makynen, J. T. Kostamovaara, and R. A. Myllyla, "Position resolution of the position-sensitive detectors in high background illumination," *IEEE Trans. Instrum. Meas.* **45**(1), 324–326 (Feb. 1996).
10. A. J. Makynen, J. T. Kostamovaara, and R. A. Myllyla, "Small angle measurement in a turbulent environment using position-sensitive detectors," in *Engineering Systems with Intelligence*, S. G. Tzafestas, Ed., pp. 275–284, Kluwer, Dordrecht (1991).
11. A. E. Siegman, *Lasers*, University Science Books (1986).

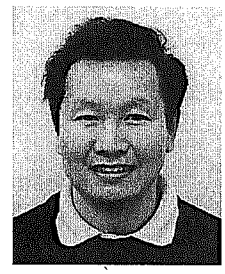

Neville K. S. Lee received his PhD in solid-state physics from MIT in 1973. He conducted research in quantum optics for MIT National Magnet Lab, laser manufacturing process for Polaroid, write-once optical storage devices for Burroughs, and memorex and magneto-optics and magnetic storage devices for Digital Equipment. He has numerous inventions and has contributed much to manufacturing technology, storage devices, lasers, optical devices, electromechanical systems, and solid-state physics. Dr. Lee is an associate professor in the Department of Industrial Engineering and Engineering Management at Hong Kong University of Science and Technology; his research interests include low-cost precision manufacturing technology, ultraprecision manufacturing systems, agile manufacturing, and management of product development.

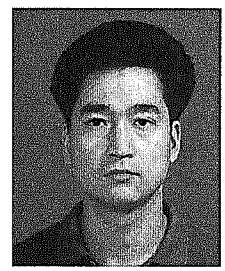

Yimin Cai obtained his first PhD in microelectronics at Southeast University, Nanjing, China, in 1994. Now he is studying for his second PhD in industrial engineering and engineering management, at Hong Kong University of Science and Technology. Dr. Cai's research interests include semiconductor devices, IC techniques, optoelectronics, precision manufacturing, and engineering management. He is a senior member of Chinese Institute of Electronics (CIE).

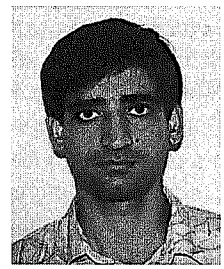

Ajay Joneja obtained his BTech in mechanical engineering from IIT, Kanpur, in 1987. He then went to study manufacturing engineering at the School of IE, Purdue University, where he received his MSIE (1989) and PhD (1993). He subsequently joined the Department of Industrial Engineering and Engineering Management at Hong Kong University of Science and Technology as an assistant professor. Dr. Joneja's research interests revolve around various aspects of manufacturing. These include CAPP, fixture planning, die machining, flexible tooling for mass customization, automatic control of manufacturing systems, and rapid prototyping.